Electronic Supplementary Material (ESI) for Nanoscale.
This journal is © The Royal Society of Chemistry 2019

Electronic Supplementary Information

Nitrogen-doped graphene fiber webs for multi-battery energy storage

Woon Gie Chong[a], Fei Xiao[b], Shanshan Yao[a], Jiang Cui[a], Zoya Sadighi[a], Junxiong Wu[a], Muhammad Ihsan-Ul-Haq[a], Minhua Shao[b], Jang-Kyo Kim*[a]

[a] Department of Mechanical and Aerospace Engineering, The Hong Kong University of Science and Technology, Clear Water Bay, Kowloon, Hong Kong

[b] Department of Chemical and Biological Engineering, The Hong Kong University of Science and Technology, Clear Water Bay, Kowloon, Hong Kong.

* Email: mejkkim@ust.hk

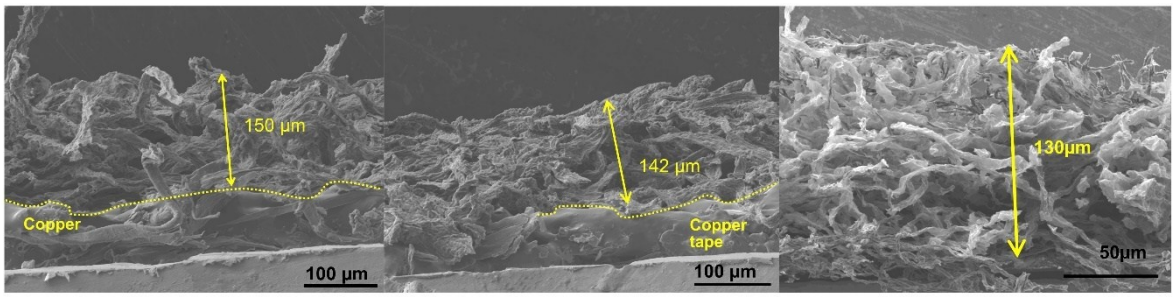

Fig. S1. Cross-sectional images of N-GFWs.

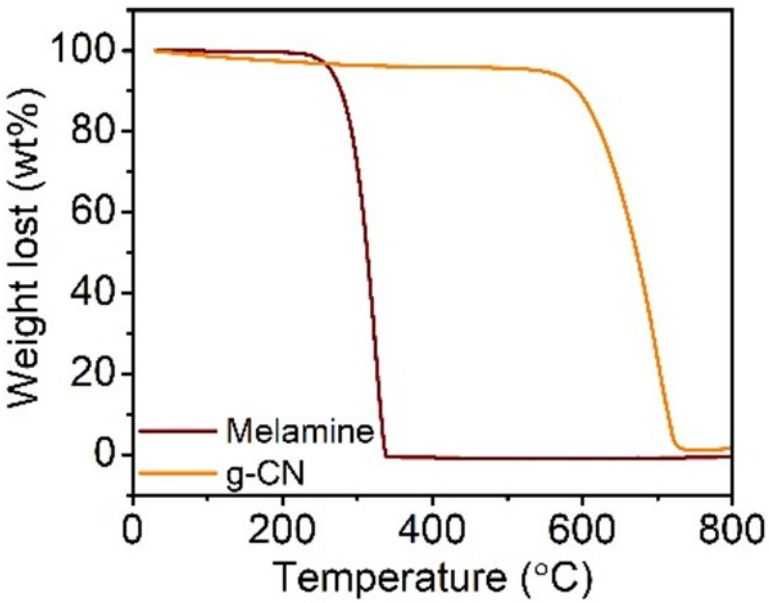

Fig. S2. TGA curves of melamine and graphitic carbon nitride (g-C_3N_4).

Fig. S3. An optical image of N-GFW900.

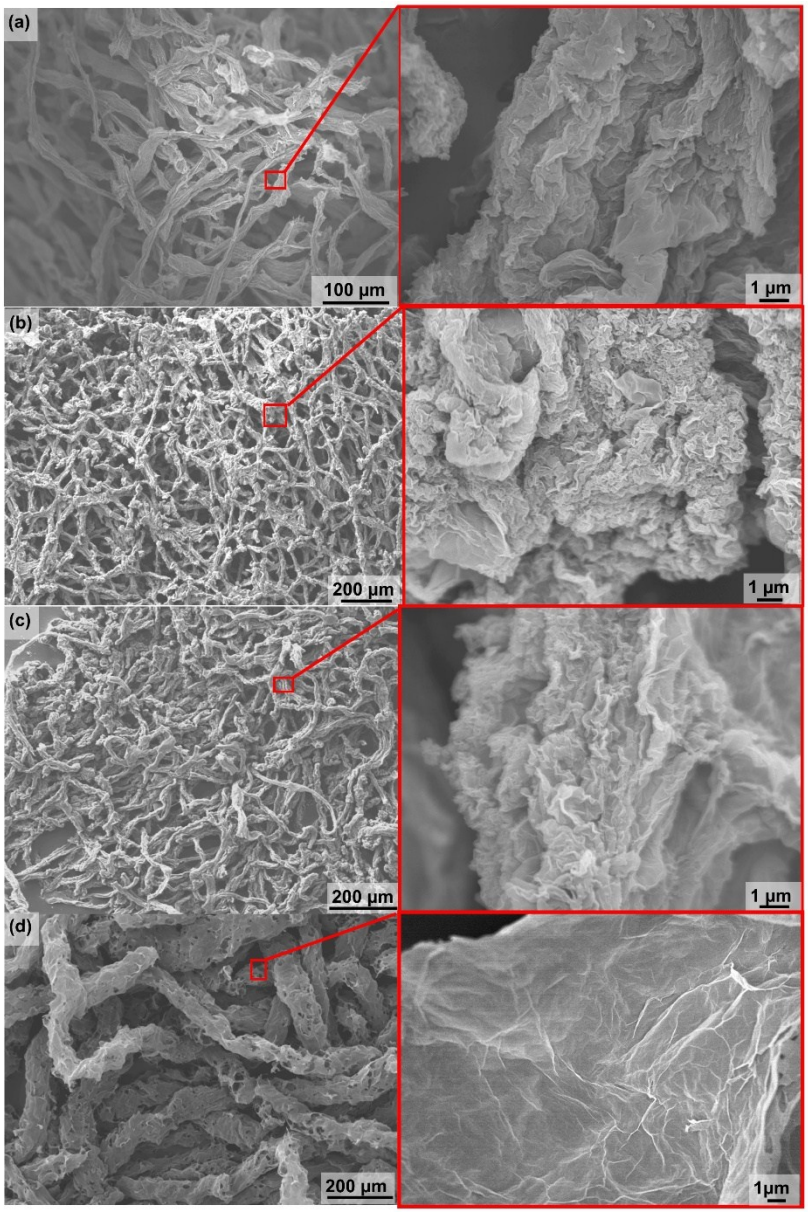

Fig. S4. SEM images of (a) GFW900 (b) N-GFW700 (c) N-GFW800 (d) freeze-dried Mel-GOFW.

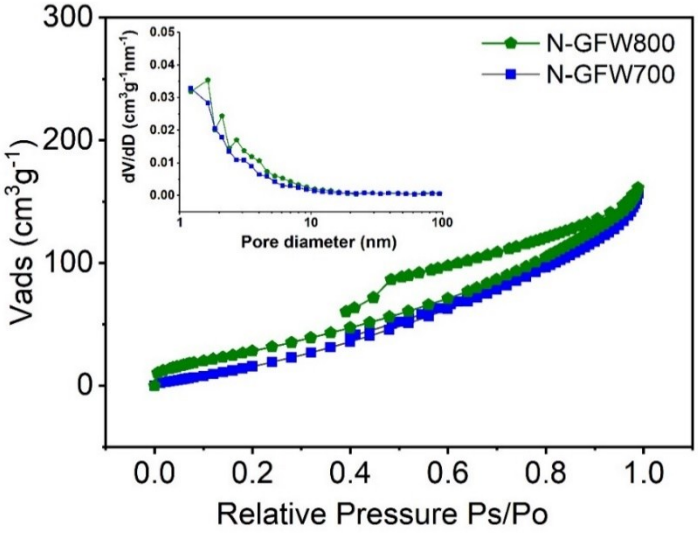

Fig. S5. Nitrogen adsorption/desorption isotherms and pore size distribution curves of N-GFW700 and N-GFW800.

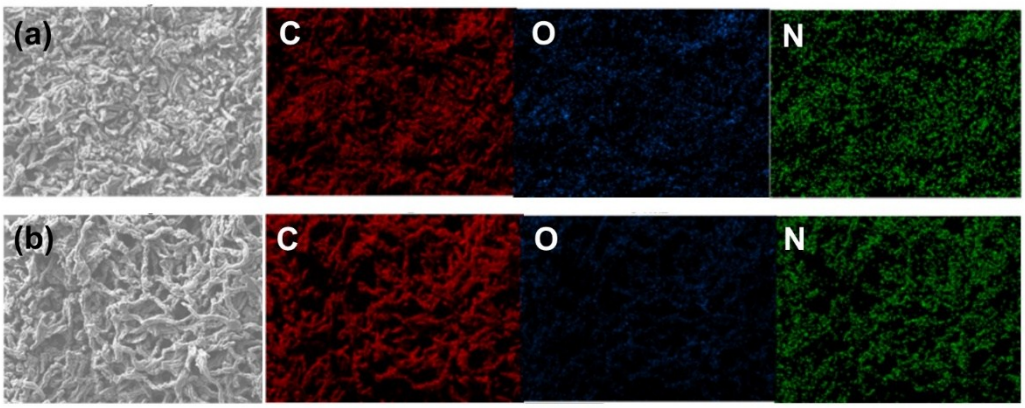

Fig. S6. EDX elemental maps of (a) N-GFW700 and (b) N-GFW800

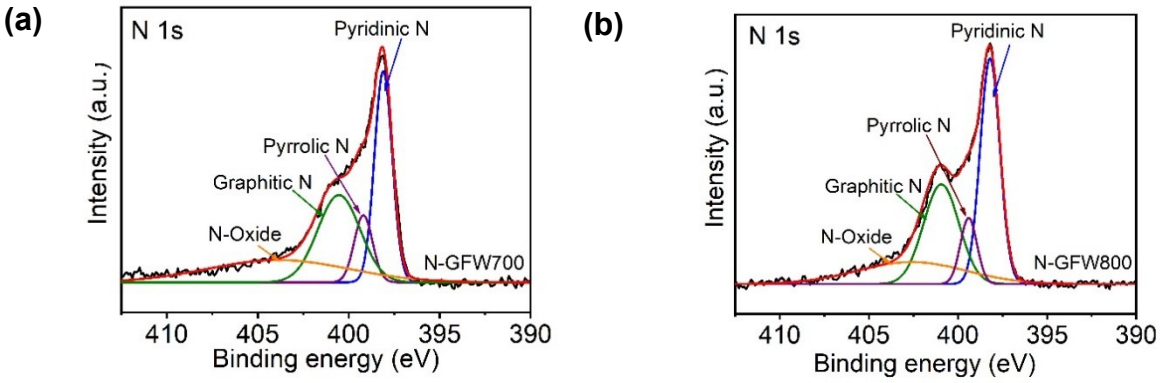

Fig. S7. Deconvoluted N 1s spectra of (a) N-GFW700 and (b) N-GFW800.

Table S1 Summary of elemental contents of GFW900 and N-GFWs.

Materials	Atomic %			Nitrogen Species			
	C	O	N	Pyridinic	Pyrrolic	Graphitic	N-oxide
GFW900	97.5	2.5	-				
N-GFW700	89.5	4.5	6.0	35.9	9.7	29.8	24.6
N-GFW800	89.8	2.9	7.3	40.8	12.9	33.4	12.9
N-GFW900	90.6	2.9	6.5	35.8	8.0	38.8	17.4

Table S2 Onset potentials and limiting currents obtained from CV and RDE measurements.

Materials	CV onset potential (V vs RHE)	ORR onset potential (V vs RHE)	Limiting current at 0.4V (mA)	OER onset potential (V vs RHE)
N-GFW700	0.652	0.594	-2.31	1.60
N-GFW800	0.657	0.568	-2.4	1.64
N-GFW900	0.678	0.556	-2.5	1.72
GFW900	0.588	0.459	-1.22	1.83

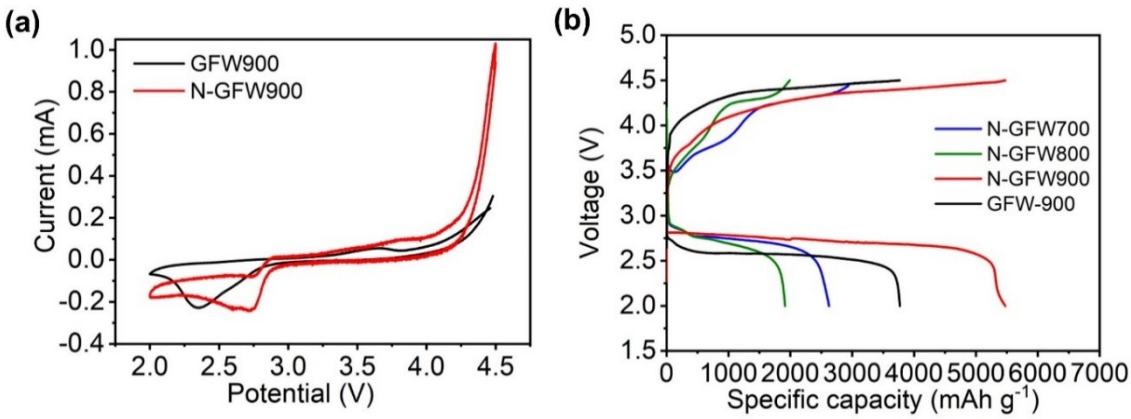

Fig. S8. (a) CV profiles of GFW900 and N-GFW900 at a scan rate of 0.1 mV s^{-1} between 2.0 and 4.5V; (b) Full GCD curves of GFW900 and N-GFWs at 100 mA g^{-1}.

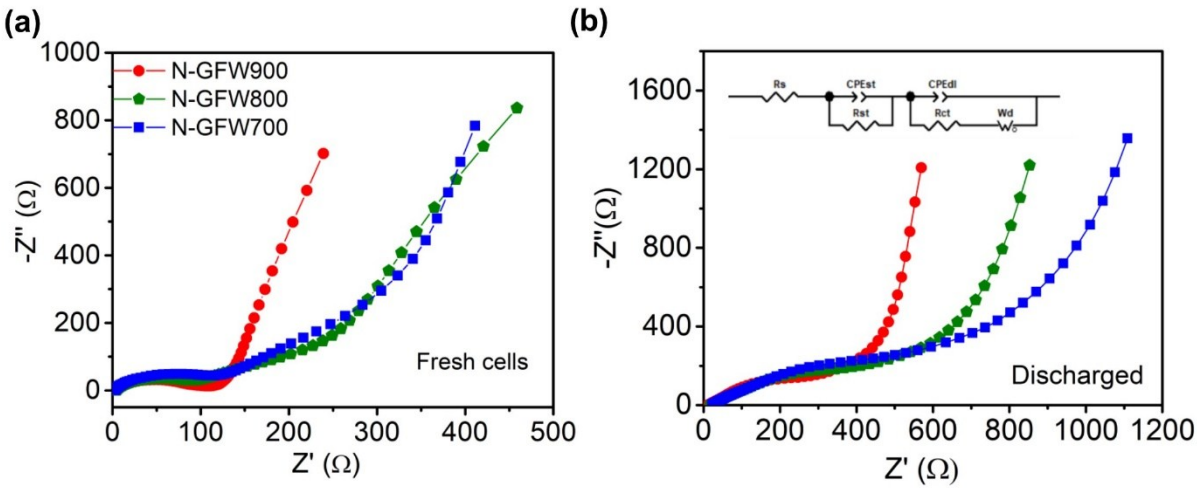

Fig. S9. EIS Nyquist diagrams of LOB with different N-GFW electrodes (a) before and (b) after the 5th discharge cycles.

Table S3 Impedance parameters of the electrodes obtained from the equivalent circuit in Fig. S9.

LOB	R_s (Ω)	R_{st} (Ω)	R_{ct} (Ω)
Fresh			
N-GFW700	4.40	101.6	9.8
N-GFW800	4.38	76.63	10.76
N-GFW900	4.63	72.0	23.5
Discharged			
N-GFW700	19.2	1001	392
N-GFW800	16.43	908.8	376
N-GFW900	12.79	635.1	115.3

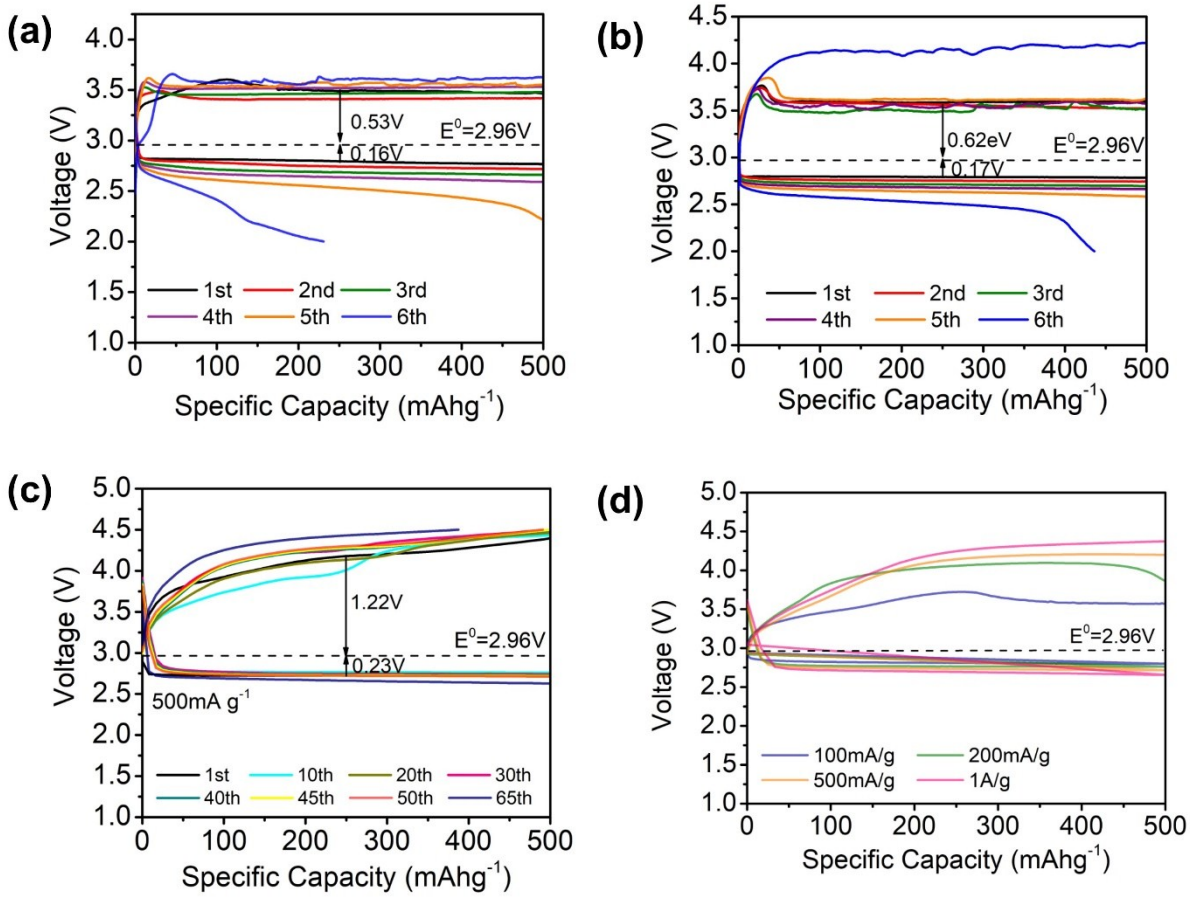

Fig. S10. GCD profiles of LOBs with (a) N-GFW700 and (b) N-GFW800 electrodes at a current density of 200 mA g^{-1} (c) N-GFW900 electrode at a current density of 500 mA g^{-1} with an upper-limit capacity of 500 mAh g^{-1}; (d) rate capability of N-GFW900 electrode measured at different current densities between 0.1 and 1A g^{-1}.

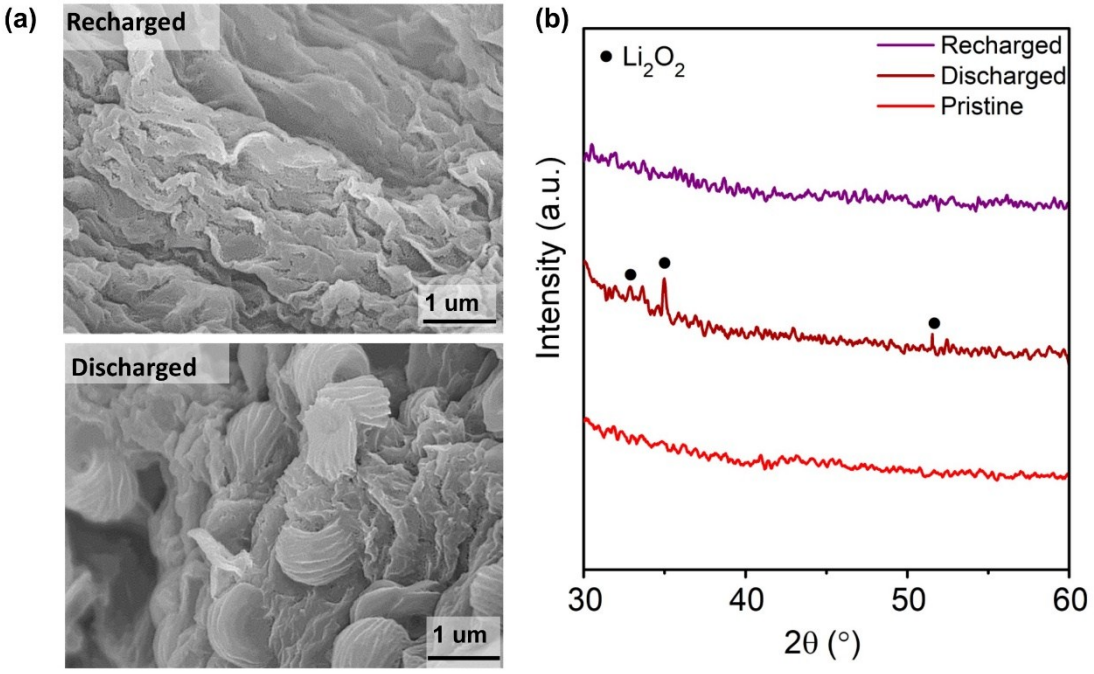

Fig. S11. *Ex situ (a)* SEM images and (b) *ex situ* XRD spectra of N-GFW900 after 50 discharge and charged cycles.

Table S4 Comparison of areal mass loadings and capacities of freestanding air cathodes between the current and previous studies.

Cathode	Cycles	Curtail Capacity (mAh g^{-1})	Current density (mA cm^{-2})	Mass loading (mg cm^{-2})	Areal Capacity (mAh cm^{-2})	Ref
3-D network GF@Al electrodes	27	1000	0.035	0.35	0.35	49
Co/CoO-graphene-carbonized melamine foam	70	500	0.25	2.45	1.2	50
N-doped graphene frameworks-PS template	54	1000	0.61	0.61	0.61	51
Dual-doped graphene and mesoporous carbon	38	1000	0.1	1	1	52
Graphene@g-C_3N_4	105	1000	0.4	2	2	53
Hierarchical-fibril CNT	65	1000	0.032	0.016	0.0161	54

Nanoporous graphene	100	500	0.23	0.23	0.115	55
Graphene oxide gel-derived porous carbon	10	2000	0.5	0.70	1.4	56
N-GFW900	60	500	0.4	2.0	1	Current work
	15	~267	0.2	7.5	2	

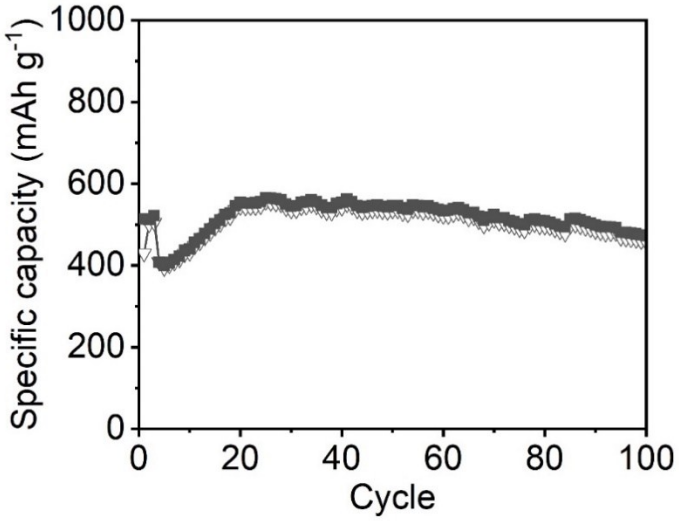

Fig. S12. Cyclic performance of LSB without an interlayer at 0.2C.

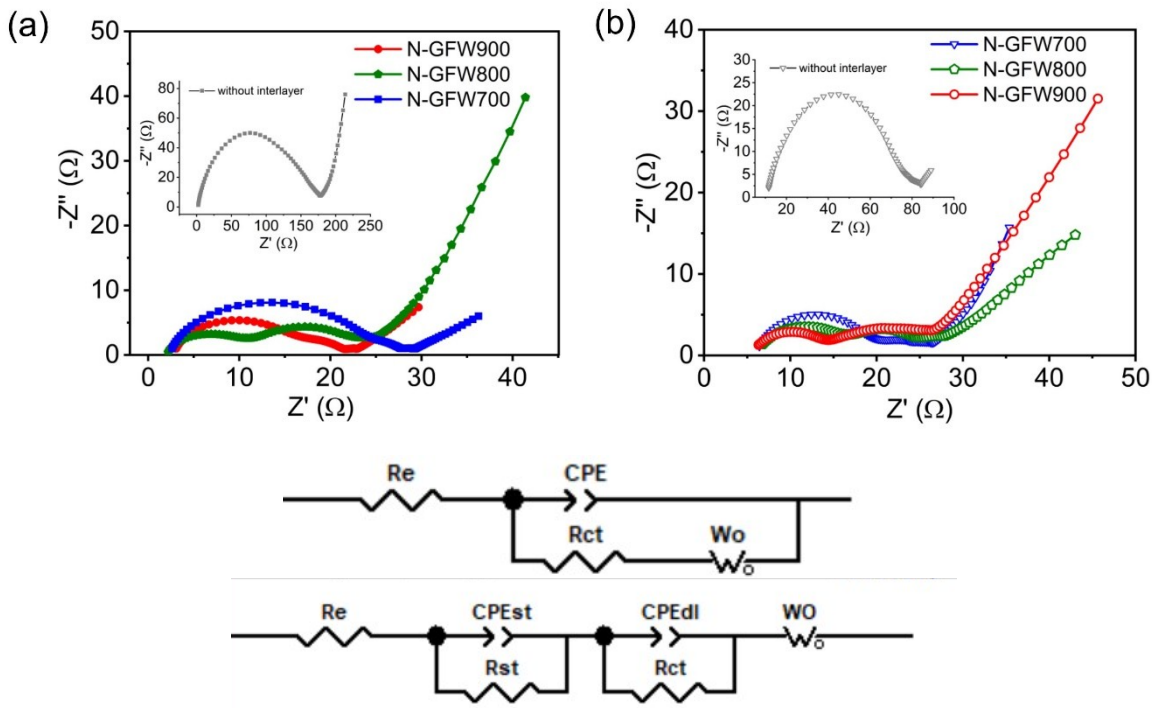

Fig. S13. EIS Nyquist plots and Z-view simulations of LSBs without and with different N-GFW interlayer (a) before (b) after cycles. R_e is the resistance of electrolyte; $R_{ct}//CPE_{dl}$ is the charge-transfer resistance; $R_{st}//CPE_{st}$ represents the interphase contact resistance; and W_o represents the diffusion resistance.

Table S5. Impedance parameters, R_e, R_{ct} and R_{st}, determined from the EIS data in Fig. S10.

LSB	R_e (Ω)	R_{ct} (Ω)	R_{st} (Ω)
Before cycle			
Without interlayer	2.8	164	-
N-GFW700	2.3	6.1	19.2
N-GFW800	2.1	7.1	12.4
N-GFW900	2.7	8.2	10.9
After 100 cycles			
Without interlayer	10.8	54.6	-
N-GFW700	6.0	5.7	12.6
N-GFW800	5.4	11	8.2
N-GFW900	5.8	9.8	10.0

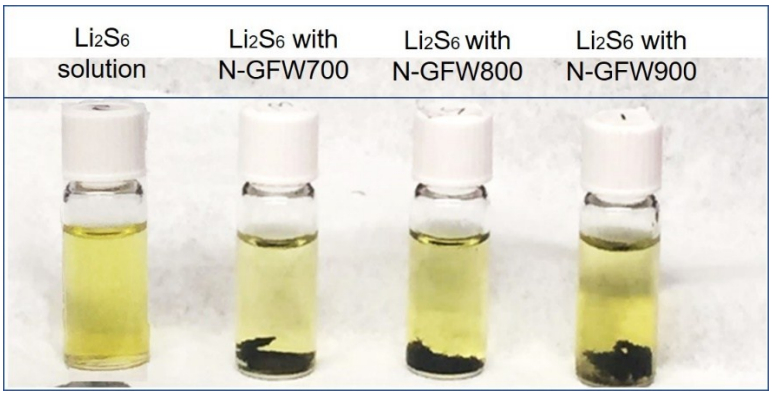

Fig. S14. Photographs of 0.001 M Li_2S_6 solution without interlayer, and with N-GFW700, N-GFW800 and N-GFW900 interlayers after 2 hr.

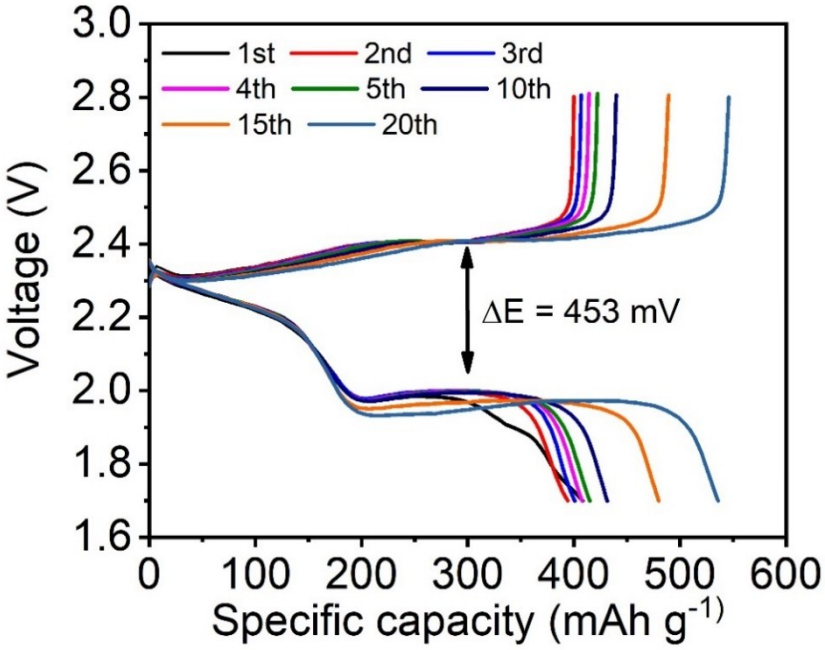

Fig. S15. GCD curves for the first 20 cycles of the LSB without interlayer at 0.2C.

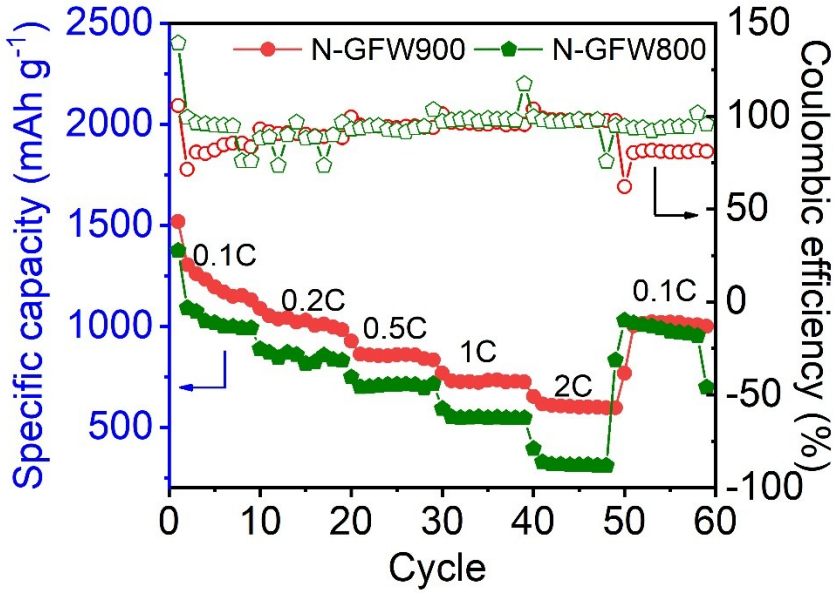

Fig. S16. Rate capabilities and the corresponding Coulombic efficiencies of LSBs with an N-GFW800 and N-GFW900 interlayer.

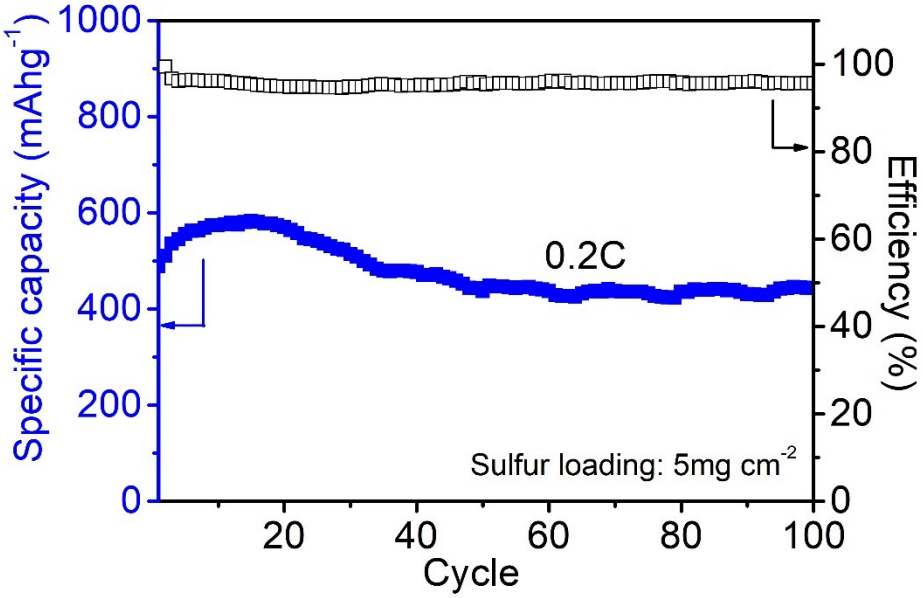

Fig. S17. Cyclic performance of the cathode containing a high sulfur loading and with an N-GFW700 interlayer.

Table S6. Comparison of electrochemical performance of LSBs with different types of interlayers

Materials	Current rate (C)	Initial discharge capacity (mAh g^{-1})	Cycle number	Residual discharge capacity (mAh g^{-1})	Decay rate (%)	Sulfur content (wt %)	Ref
PAA-SWCNT film	1	770	200	573	0.13	54	68
3D-NG film	0.5	800	200	530	0.17	70	69
Nickel foam	0.2	819	80	604	0.32	60	70
Fe_3C/CNF	0.12	1177	100	893	0.24	70	S[1]
GO/carbon black	0.1	1260	100	894	0.29	80	S[2]
Carbon fiber monolith	0.2	1120	100	630	0.44	60	S[3]
Cellulose/GO	0.18	2736	200	474	0.41	80	S[4]
Acetylene black	0.1	1491	50	1062	0.58	60	S[5]
Carbon paper	0.2	1500	50	810	0.92	70	S[6]
MWCNT	0.5	1446	100	855	0.41	70	59
Microporous carbon paper	1	1176	100	1000	0.15	70	S[7]
GO/CNT	0.2	1370	300	671	0.17	70	57
MoS_2/CNT	0.2	1237	500	648	0.061	50	71
SnO_2/RGO	1	1026	200	734	0.14	55	72
Carbonized CWF	0.1	1346.9	100	1076.6	0.2	70	S[8]
MoP_2/CNT Film	0.2	1223	100	905	0.152	50	S[9]
Functional CNF	0.2	1356	100	917	0.16	70	S[10]
N-GFW700	0.2	810	100	663	0.18	70	Current study
	0.5	658.8	200	605	0.04	70	

PAA = poly(acrylic acid)
SWCNT = single walled CNT
NG = N-doped graphene
RGO = reduced graphene oxide
CWF = cotton weave fabric
MoP_2 = Molybdenum diphosphide

References

S [1] J. Huang, B. Zhang, Z. Xu, S. Abouali, M. A. Garakani, J. Huang and J.K. Kim*, J. Power Sources,* 2015, **285**, 43-50.

S [2] X. Wang, Z. Wang and L. Chen, *J. Power Sources*, 2013, **242**, 65-69.

S [3] L. Zhang, Y. Wang, B. Peng, W. Yu, H. Wang, T. Wang, B. Deng, L. Chai, K. Zhang and J. Wang, *Green Chem.*, 2014, **16**, 3926-3934.

S [4] Q. Zheng, X. Leng, K. Wu, I.R. Gentle and D. Wang, *Carbon,* 2015, **93**, 611-619.

S [5] T. Jeong, Y. H. Moon, H. Chun, H. S. Kim, B. W. Cho and Y. Kim, *Chem. Commun.*, 2013, **49**, 11107-11109.

S [6] K. Zhang, Q. Li, L. Zhang, J. Fang, J. Li, F. Qin, Z. Zhang and Y. Lai, *Mater Lett.*, 2014, **121**, 198-201.

S [7] Y. Su and A. Manthiram, *Nat. Commun.,* 2012, **3**, 1166.

S [8] Q. Zhao, Q. Zhu, Y. An, R. Chen, N. Sun, F. Wu and B. Xu, *Appl. Surf. Sci.,* 2018, **440**, 770-777.

S [9] Y. Luo, N. Luo, W. Kong, H. Wu, K. Wang, S. Fan, W. Duan and J. Wang, *Small,* 2018, **14**, 1702853.

S [10] K. Wu, Y. Hu, Z. Shen, R. Chen, X. He, Z. Cheng and P. Pan, *J. Mater. Chem. A*, 2018, **6**, 2693-2699.